Packaged BiCMOS Embedded RF-MEMS Switches with Integrated Inductive Loads

M. Kaynak[1], M. Wietstruck[1], W. Zhang[1], J. Drews[1], R. Barth[1], D. Knoll[1], F. Korndörfer[1], R. Scholz[1], K. Schulz[1], C. Wipf[1], B. Tillack[1,2], K. Kaletta[3], M. v. Suchodoletz[3], K. Zoschke[3], M. Wilke[3], O. Ehrmann[3], A. C. Ulusoy[4], T. Purtova[4], G. Liu[4], H. Schumacher[4]

[1]IHP, Im Technologiepark 25, 15236 Frankfurt Oder, Germany, Email: kaynak@ihp-microelectronics.com
[2]Technische Universität Berlin, HFT4, Einsteinufer 25, 10587, Berlin, Germany
[3]Fraunhofer IZM, Gustav-Meyer-Allee 25, 13355 Berlin, Germany
[4]Institute of Electron Devices and Circuits, Ulm University, Albert-Einstein-Allee 45, 89081 Ulm, Germany

ABSTRACT — **This paper presents packaged BiCMOS embedded RF-MEMS switches with integrated inductive loads for frequency tuning at mm-wave frequencies. The developed technique provides easy optimization to maximize the RF performance at the desired frequency without having an effect on the switch mechanics. Insertion loss less than 0.25 dB and isolation better than 20 dB are achieved from 30 to 100 GHz. A glass cap with a silicon frame is used to package the switch. Single-pole-double-throw (SPDT) switches and a 24 – 77 GHz reconfigurable LNA is also demonstrated as a first time implementation of single chip BiCMOS reconfigurable circuit at such high frequencies.**

Index Terms **— BiCMOS, millimeter wave integrated circuits, packaging, microelectromechanical devices , RFMEMS, switches.**

I. INTRODUCTION

Latest developments in RF-MEMS switch technology have paved the way to use mechanical switches, in particular capacitive ones in mm-wave applications such as satellite and space communication (30 – 50 GHz), E-band communication (60 – 90 GHz), and imaging systems (94 GHz) [1]-[4]. Nowadays, RF-MEMS technologies have become more mature and commercial products can be found, especially focused on frequency bands lower than 40 GHz [5]-[7]. For all these applications, low insertion loss and high isolation of the switch at different center frequencies are key requirements and can be achieved by tuning the resonance frequency of the capacitive switch in the down-state. The typical method in use for frequency tuning of capacitive type RF-MEMS switches is changing the contact capacitance, which, however, leads to a change in the mechanics of the system [8]. There are two obvious disadvantages of this method. Firstly, optimizing the mechanics for any new frequency band needs effort and is very time consuming. Secondly, every change in the system mechanics requires repetitions of reliability and qualification tests, making the development very cost intensive.

In this paper, we demonstrate an integrated inductive loading technique to tune the operating frequency of a BiCMOS embedded, capacitive RF-MEMS switch. The developed technique provides a wide range frequency tuning from 30 GHz to 100 GHz with excellent performance parameters beyond state of the art silicon based switches [9]–[14]. Switches with same mechanics are optimized for four center frequencies (30, 50, 80, and 100 GHz) to demonstrate the feasibility of the technique. An improved RF signal line together with inductive loading technique provides less than 0.25 dB insertion loss and better than 20 dB isolation in each frequency band. A glass cap with a silicon frame is also developed and capped to the RF-MEMS switch using non-conductive polyimide to prevent from package losses. No performance degradation was observed after the packaging process. SPDT switches for different frequency bands and a reconfigurable (24–77 GHz) LNA are also demonstrated using the developed frequency scalable RF-MEMS switches.

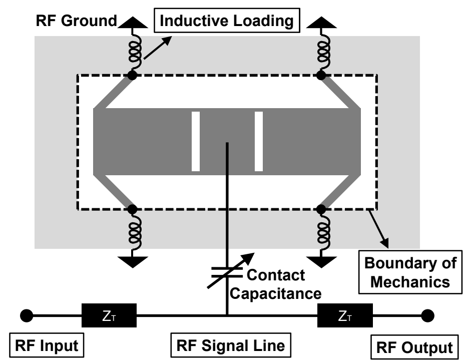

Fig. 1 Concept of inductive loading. Additional inductors are out of mechanical boundary (in BEOL oxide) and have no effect on the mechanics of the movable membrane.

II. TECHNOLOGY

Fig. 1 illustrates the concept of the inductive loading technique, which was applied to the BiCMOS embedded RF-MEMS switch described in [13]. The additional inductors, realized in the BiCMOS BEOL, were added between the movable membrane and the RF ground ring to change the total inductance to ground. It results in a change of switch resonance frequency without having an effect on the switch mechanics. Fig. 2 shows the realized switches for four different frequency bands with the same movable membranes but different inductive loads. The surrounding RF ground ring is formed by stacking all available metallization layers and is connected to the silicon substrate through contact vias.

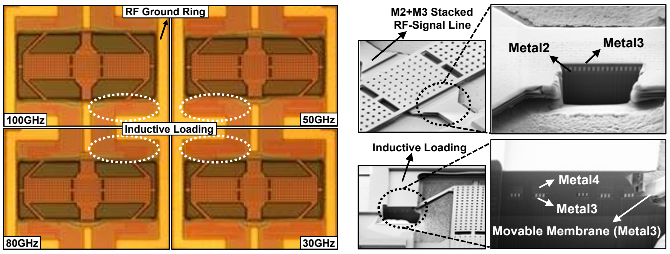

Fig. 2 Microphotographs of RF-MEMS switches for four different frequencies: 100, 80, 50, and 30 GHz (Left). Signal line and additional inductor: M2+M3 stacked layer is used as signal line except contact region. Additional inductors are realized using M3+M4 stack to increase the Q-factor of the inductor (Right).

The switch insertion loss was significantly lowered compared to a former version [13] by optimizing the RF line width and stacking the Metal2 (M2) and Metal3 (M3) layers in the region outside of the contact region where most of the resistive loss originates. The maximum isolation is mainly limited by the Q-factor of the additional inductors. Therefore, the inductor spirals were formed by stacking M3 and Metal4 (M4) layers (Fig. 2).

Due to the very robust and excellent reliable operation of the switch in ambient environment [15], a non-hermetic type of package from a glass cap is chosen in order to protect the RF performance (Fig.3a). The upside down view of the glass cap is given in Fig. 3b. The cap fabrication process starts with bonding of a glass wafer to a silicon wafer and polishing the silicon wafer down to 50 µm thickness. The silicon frames (Fig.3b) are formed by deep reactive ion etching with a final thickness of 50 µm and a width of 30 µm. Then, the polyimide adhesive is applied to the silicon frame surface and glass caps are diced. Lastly, a cap-to-wafer packaging is performed with a temperature of less than 300˚C, compatible with the underlying BiCMOS structures. No significant change in the mechanics was observed after packaging (Fig. 3c).

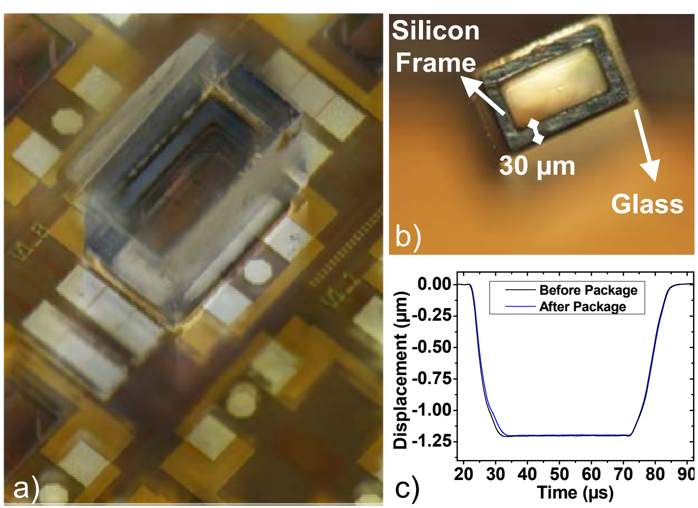

Fig. 3 a) View of a packaged switch with glass cap, b) Silicon frame on the bottom of glass package, c) Switch displacement (contact region) versus time curves before and after package (through glass) by Laser-Doppler Vibrometer.

III. Results

Fig. 4 shows the performance parameters of the RF-MEMS switches optimized for 30, 50, 80 and 100 GHz, respectively. For both cases, the insertion loss (IL) is less than 0.25 dB, while the isolation (ISO) is better than 20 dB in the targeted frequency bands. The lowest insertion losses of all investigated RF signal line variants were achieved for a signal line width of 30 µm, except at 100 GHz. For this case, a width of 20 µm proved to be the best, due to the substrate coupling loss which increases with higher frequencies. Fig. 4 also demonstrates that increasing the inductive loads Q-factor by metal layers stacking (M3+M4) improves the isolation by more than 5 dB in all cases.

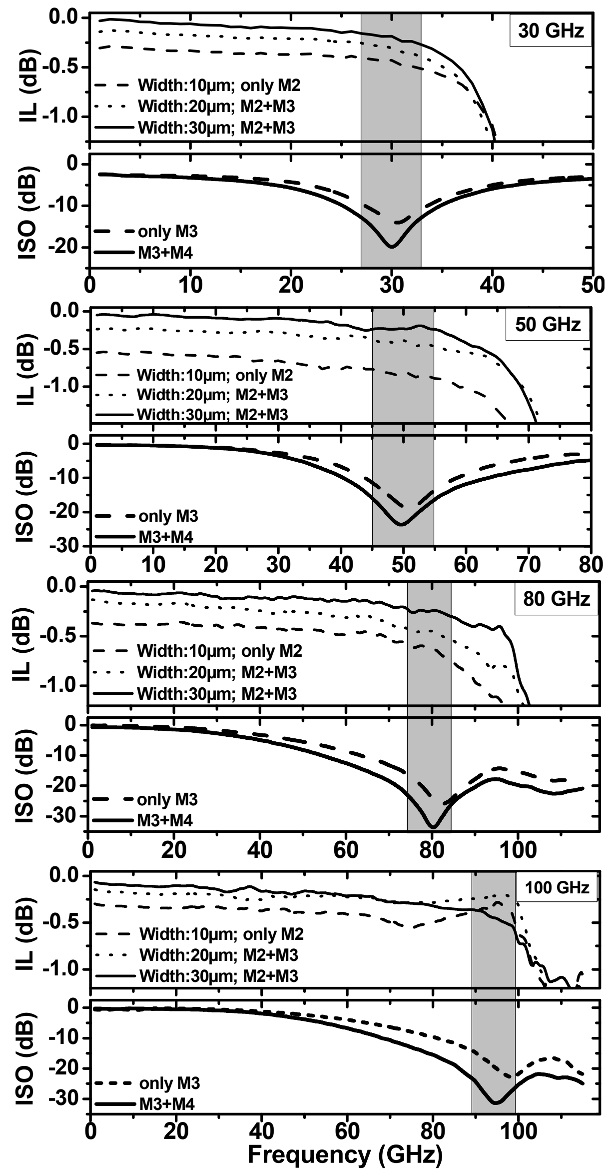

Fig. 4 Measured (De-embedded) insertion loss and isolation of RF-MEMS switches with different signal line conditions and different inductor metal stacks. Measurements are average of >60 switch over an 8-inch substrate. Targeted operation bands are gray marked.

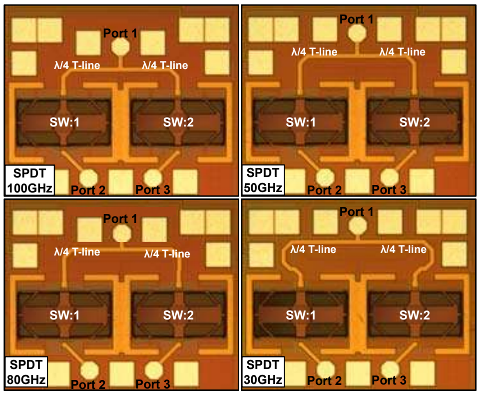

Fig. 5 Microphotographs of SPDTs for 100, 80, 50, and 30 GHz. Every SPDT uses corresponding RF-MEMS switch.

IV. Design Examples

As a proof of concept, SPDT switches for different frequency bands were designed using the developed switches. The SPDTs were formed by two quarter-wavelength transmission lines terminated by the RF-MEMS switches (Fig. 5). The SPDTs show excellent RF performance parameters, such as less than 1 dB insertion loss and better than 20 dB isolation (Fig. 6). The achieved results are far beyond those of state of the art SPDTs based on silicon technology [16]-[18] and can be improved in future designs by further optimization on transmission lines.

In addition to the passive SPDTs, a 24–77 GHz reconfigurable two stage LNA was designed where two switches were used to change the length of the load transmission lines (Fig. 7a). Peak gains of more than 25 dB and 20 dB were measured for two different states at 24 GHz and 72 GHz, respectively (Fig. 7b). The noise figure at 72 GHz, where the RF-MEMS switch is in down-state, was measured as 8 dB. The performance distribution of the LNA over 8-inch wafer is given in Fig. 7b with gray curves. The small variance shows the good uniformity of the BiCMOS embedded MEMS process.

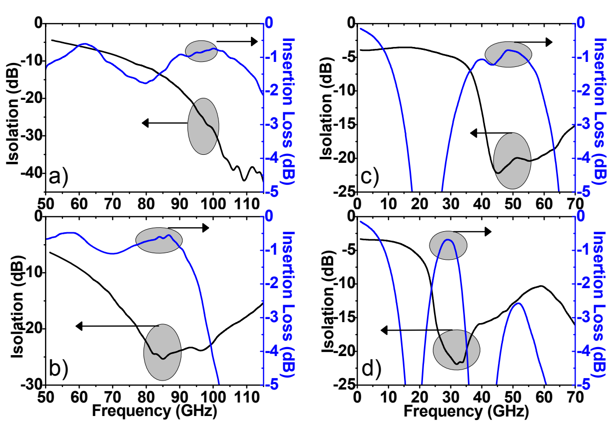

Fig. 6 Measured (De-embedded) S-parameters of SPDTs tuned for a) 100 GHz, b) 80 GHz, c) 50 GHz, and d) 30 GHz: Insertion loss between Port1 and Port2 (SW1 up-state, SW2 down-state), isolation between Port1 and Port2 (SW1 down-state, SW2 up-state).

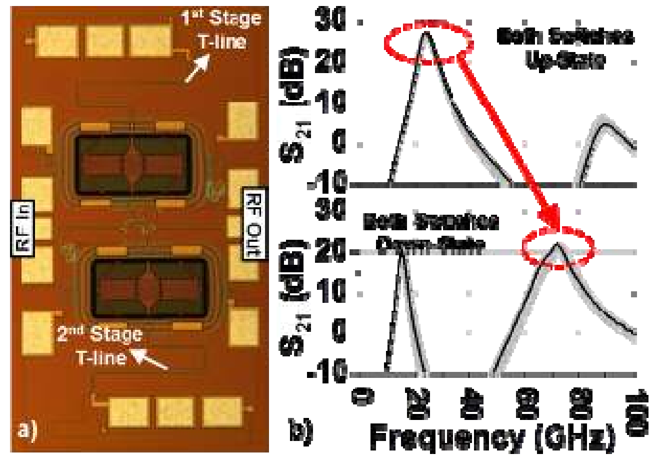

Fig. 7 a) View of 24–77 GHz reconfigurable 2-stage LNA, b) S_{21} vs. frequency for the different states with variation of >45 samples over an 8-inch substrate. (Black curve shows average)

V. Conclusion

Integrated inductive loads for frequency tuning of RF-MEMS switches have been successfully demonstrated at mm-wave frequencies. The developed technique provides easy optimization to maximize the RF performance at the desired frequency without having an effect on the switch mechanics. A glass cap with a silicon frame was used to package the switch and no performance degradation was observed after packaging process. SPDTs for four different frequency bands with excellent parameters were demonstrated using the developed technique. A 24-77 GHz reconfigurable LNA was also demonstrated as a first time implementation of single chip BiCMOS reconfigurable circuit at such high frequencies. The excellent reliability of BiCMOS embedded RF-MEMS switch [15], together with the developed packaging and inductive loading techniques make the presented RF-MEMS switch feasible to use as a key component for single chip high performance mm-wave reconfigurable silicon RFICs.

References

[1] E. R. Brown, IEEE MTT., vol.46, p. 1868, 1998.
[2] G. M. Rebeiz, J. Muldavin, IEEE Mic. Mag., vol.2, p. 59, 2001.
[3] R. R. Mansour, Proceedings of ICMENS, p. 191, 2005.
[4] O. Vendier, et al., Proceedings of EuMC, p. 807, 2006.
[5] Radant MEMS, Inc., http://www.radantmems.com
[6] WiSpry, Inc., http://www.wispry.com
[7] MEMtronics Corporation, http://www.memtronics.com
[8] V. Puyal, et al., TMTT, vol.57, p.2824, 2009.
[9] A. Akiba, et al., IEDM Technical Digest, p. 36.4.1-36.4.4, 2010.
[10] T. Yamamoto, et al., Proceedings of APMC, p. 198-201, 2009.
[11] Y.S.Lee, et al., Proceedings of MEMS2010, p. 759-762, 2010.
[12] A. Stehle, et al., Proceedings of EUMC2008, p., 104-107, 2008.
[13] M. Kaynak, et al., IEDM Technical Digest, p. 797, Dec. 2009.
[14] M. Kaynak, et al., IEDM Technical Digest, p. 832-835, Dec. 2010.
[15] M. Kaynak, et al., SiRF Technical Digest, p. 177, 2011.
[16] M. Uzunkol, et al., JSSC, vol. 45, p. 2003-2007, 2010.
[17] S. F. Chao, et al., LMWC, vol.17, p. 130-132, 2007.
[18] T. Quemerais, et al., Proceedings of EUMC, p. 425, 2010.

978-1-4673-1088-8/12/$31.00 ©2012 IEEE